



This is a repository copy of *The role of multiplicative complexity in compiling Low T-count Oracle circuits*.

White Rose Research Online URL for this paper:  
<http://eprints.whiterose.ac.uk/156758/>

Version: Accepted Version

---

**Proceedings Paper:**

Meuli, G., Soeken, M., Campbell, E. et al. (2 more authors) (2019) The role of multiplicative complexity in compiling Low T-count Oracle circuits. In: 2019 IEEE/ACM International Conference on Computer-Aided Design (ICCAD). 2019 IEEE/ACM International Conference on Computer-Aided Design (ICCAD), 04-07 Nov 2019, Westminster, CO, USA. IEEE . ISBN 9781728123516

<https://doi.org/10.1109/iccad45719.2019.8942093>

---

© 2019 IEEE. Personal use of this material is permitted. Permission from IEEE must be obtained for all other users, including reprinting/ republishing this material for advertising or promotional purposes, creating new collective works for resale or redistribution to servers or lists, or reuse of any copyrighted components of this work in other works. Reproduced in accordance with the publisher's self-archiving policy.

**Reuse**

Items deposited in White Rose Research Online are protected by copyright, with all rights reserved unless indicated otherwise. They may be downloaded and/or printed for private study, or other acts as permitted by national copyright laws. The publisher or other rights holders may allow further reproduction and re-use of the full text version. This is indicated by the licence information on the White Rose Research Online record for the item.

**Takedown**

If you consider content in White Rose Research Online to be in breach of UK law, please notify us by emailing [eprints@whiterose.ac.uk](mailto:eprints@whiterose.ac.uk) including the URL of the record and the reason for the withdrawal request.



[eprints@whiterose.ac.uk](mailto:eprints@whiterose.ac.uk)  
<https://eprints.whiterose.ac.uk/>

# The Role of Multiplicative Complexity in Compiling Low $T$ -count Oracle Circuits

Giulia Meuli<sup>1</sup> Mathias Soeken<sup>1</sup> Earl Campbell<sup>2</sup> Martin Roetteler<sup>3</sup> Giovanni De Micheli<sup>1</sup>

<sup>1</sup>Integrated Systems Laboratory, EPFL, Lausanne, CH

<sup>2</sup>Department of Physics and Astronomy, University of Sheffield, Sheffield, UK

<sup>3</sup>Microsoft, Redmond, US

**Abstract**—We present a constructive method to create quantum circuits that implement oracles  $|x\rangle|y\rangle|0\rangle^k \mapsto |x\rangle|y \oplus f(x)\rangle|0\rangle^k$  for  $n$ -variable Boolean functions  $f$  with low  $T$ -count. In our method  $f$  is given as a 2-regular Boolean logic network over the gate basis  $\{\wedge, \oplus, 1\}$ . Our construction leads to circuits with a  $T$ -count that is at most four times the number of AND nodes in the network. In addition, we propose a SAT-based method that allows us to trade qubits for  $T$  gates, and explore the space/complexity trade-off of quantum circuits.

Our constructive method suggests a new upper bound for the number of  $T$  gates and ancilla qubits based on the multiplicative complexity  $c_{\wedge}(f)$  of the oracle function  $f$ , which is the minimum number of AND gates that is required to realize  $f$  over the gate basis  $\{\wedge, \oplus, 1\}$ . There exists a quantum circuit computing  $f$  with at most  $4c_{\wedge}(f)$   $T$  gates using  $k = c_{\wedge}(f)$  ancillae. Results known for the multiplicative complexity of Boolean functions can be transferred.

We verify our method by comparing it to different state-of-the-art compilers. Finally, we present our synthesis results for Boolean functions used in quantum cryptanalysis.

## I. INTRODUCTION

Quantum computing exploits quantum phenomena such as superposition, entanglement, and interference, in order to provide superior computational capabilities. Many quantum algorithms have been proposed that promise computational speed-ups, e.g., Grover’s algorithm [1] for satisfiability checking, Shor’s algorithm [2] for factoring, and the HHL algorithm [3] for solving linear equations.

The computations performed by a quantum computer can be characterized in terms of unitary matrix operations. In order to implement them on a physical quantum device, they must be expressed in terms of the supported quantum gate library, that is a set of small unitary matrices. In fault tolerant quantum computing, the gate library includes the single-qubit gates  $H$  (Hadamard),  $S$  (phase), and  $T$  gate, as well as the 2-qubit CNOT gate. The gates  $H$ ,  $S$ , and CNOT are called Clifford gates, and their execution is significantly less expensive compared to the  $T$  gate. Thus, it is customary to only count the number of  $T$  gates ( $T$ -count) when costing a quantum computation [4].

A quantum circuit is a sequence of gates to be executed on a quantum computer in order to perform a quantum algorithm. Oracle circuits, that implement the abstract unitary operation  $U_f$  for some Boolean function  $f : \{0, 1\}^n \rightarrow \{0, 1\}$ , play an important role in many quantum algorithms, e.g., Grover’s algorithm [1]. In fault tolerant quantum computing, the quality

of an oracle circuit is measured in the  $T$ -count of the quantum circuit and the number of helper qubits (ancillae) required in order to perform the computation.

Quantum compilation is the task of decomposing abstract unitary operations into quantum circuits. In this paper, we present a constructive compilation algorithm that finds a quantum circuit for the oracle  $U_f$ , minimizing the number of  $T$  gates. The input function  $f$  is represented as a 2-regular Boolean logic network over the gate basis  $\{\wedge, \oplus, 1\}$ , i.e., it consists only of 2-input AND gates, 2-input XOR gates, and can have constant-1 inputs (0-input gate). The construction leads to a quantum circuit consisting of Clifford gates, and at most  $2\bar{c}$  Toffoli gates, where  $\bar{c}$  is the number of AND gates in the logic network for  $f$ .

The multiplicative complexity  $c_{\wedge}(f)$  of a Boolean function  $f$  is the minimum number of AND gates that is required to implement it over the gate basis  $\{\wedge, \oplus, 1\}$  [5]. The multiplicative complexity of a circuit is the number of AND gates, and therefore an upper bound for the multiplicative complexity of the function it represents. Our proposed compilation method immediately leads to an upper bound on the number of  $T$  gates in a quantum circuit that computes  $U_f$ : each AND gate is translated into a pair of 2 Toffoli gates that can be realized using special computation and uncomputation circuits, requiring 4 and 0  $T$  gates respectively [6], [7]. More details about this implementation of the quantum AND gate are given in Section II-D. It follows that, to implement  $U_f$ , at most  $4c_{\wedge}(f)$   $T$  gates and  $c_{\wedge}(f)$  extra qubits are required. Computing the multiplicative complexity for an arbitrary Boolean function is intractable [8]. Nevertheless, many heuristic algorithms have been proposed to minimize the multiplicative complexity of Boolean circuits [9], [10], [11], [12]—almost exclusively motivated by applications in cryptography. In fact, for some classes of Boolean functions the exact multiplicative complexity is known, e.g., all Boolean functions with up to 6 inputs [12] and all symmetric Boolean functions [9].

We compare the proposed compilation method with a state-of-the-art hierarchical method based on the Bennett clean-up strategy [13], which aims at reducing the number of  $T$  gates and relies on many extra qubits [14]. To make the comparison fair, we modify the state-of-the-art technique to also implement the quantum AND gate with 4  $T$  gates.

Our experimental comparison demonstrates how our proposed method returns the same number of  $T$  gates than the state-of-the-art approach, but 70% fewer qubits on average.

In a second evaluation, we compare against the *best-fit* LUT-based compilation method which aims at reducing the number of qubits [15]. Our method generates circuits with more qubits, but with  $20.4\times$  fewer  $T$  gates on average, for the considered benchmarks. The contributions of this work are:

- we identify the connection between the multiplicative complexity of Boolean functions  $c_\wedge(f)$  and the number of qubits and  $T$ -count of a quantum oracle for  $f$ ;
- we introduce xor-and inverter graphs (XAG) as a suitable multi-level logic representation for the synthesis of quantum oracles;
- we propose a constructive compilation algorithm that reaches the upper bound of  $4 \cdot c_\wedge(f)$   $T$  gates;
- we present a SAT-based reversible pebbling method that acts on XAG networks and allows us to trade qubits for gates, as the number of ancilla qubits may be imposed by the quantum computing device;
- finally, we provide synthesis results for Boolean functions that could be applied in quantum cryptography.

## II. PRELIMINARIES

### A. Quantum states

While classical computing processes bits, which can be in one of the two “classical” logic states 0 and 1, quantum computing acts on qubits, which can be in any superposition of the classical states.

The state  $|q\rangle$  of a qubit  $q$  is represented by a linear combination of the classical states,  $|q\rangle = \alpha|0\rangle + \beta|1\rangle = \begin{pmatrix} \alpha \\ \beta \end{pmatrix}$ , with  $\alpha, \beta \in \mathbb{C}$  and  $|\alpha|^2 + |\beta|^2 = 1$ . For example, the classical states are represented by  $|0\rangle = \begin{pmatrix} 1 \\ 0 \end{pmatrix}$  and  $|1\rangle = \begin{pmatrix} 0 \\ 1 \end{pmatrix}$ . A quantum state can be represented by a point on the surface of the Bloch sphere, in which the poles represent the two classical logic states. The points on the surface of the sphere are all possible superposed states. For example, all states on the equator of the sphere represent the states with  $|\alpha|^2 = |\beta|^2 = \frac{1}{2}$ , characterized by different angles with respect to the  $z$ -axis. While a single-qubit system is characterized by two complex coefficients, a 2-qubit system requires 4 complex coefficients to be represented. In general, to characterize the state of  $n$  qubits and to simulate the quantum system behavior on a classical computer,  $2^n$  complex coefficients are required.

### B. Quantum operations

The state of a qubit can be modified by applying quantum operations. All quantum operations that act on  $n$  qubits can be represented by  $2^n \times 2^n$  unitary matrices. Quantum devices are operated by means of sets of particular unitary matrices, called quantum gate libraries. In this work, we target the following operations that are customary when addressing fault tolerant quantum computing: Clifford operations ( $H$ , CNOT,  $S$ ) and

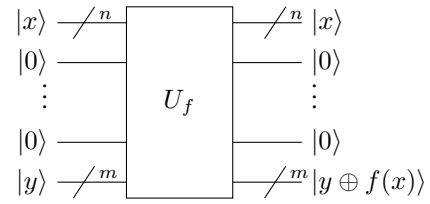


Fig. 1. Quantum circuit performing the oracle  $U_f$  of a generic multi-input multi-output Boolean function  $f$ .

the non-Clifford  $T$  operation. The matrices of the Clifford+ $T$  group are:

$$H = \frac{1}{\sqrt{2}} \begin{pmatrix} 1 & 1 \\ 1 & -1 \end{pmatrix}, \text{CNOT} = \begin{pmatrix} 1 & 0 & 0 & 0 \\ 0 & 1 & 0 & 0 \\ 0 & 0 & 0 & 1 \\ 0 & 0 & 1 & 0 \end{pmatrix},$$

$$S = \text{diag}(1, i), T = \text{diag}(1, e^{i\pi/4}). \quad (1)$$

The group also includes the quantum NOT gate  $X = HS^2H = \begin{pmatrix} 0 & 1 \\ 1 & 0 \end{pmatrix}$ . These gates abstract operations on the physical level. For example, the non-Clifford  $T$  gate is injected to the circuit through a process called magic-state distillation [16]. Many rounds of distillation are required to reach a reasonable error rate (about  $10^{-12}$ ). It has been shown how, when performing error correction, the  $T$  gate results to be more expensive than Clifford gates, independently from the desired error rate [17].  $T$  gates are generally considered about  $50\times$  more expensive than Clifford gates, in fault tolerant quantum computing.

Computation on a multi-qubit system is modelled by a quantum circuit, which represents a program (set of operations) performed in succession on different qubits. Quantum circuits are characterized by three main parameters: (i) number of qubits, (ii) number of gates and (iii) circuit depth. As we already explained,  $T$  gates are the most expensive gate in fault tolerant quantum computing. For this reason, we also define: the  $T$ -count (number of  $T$  gates) and the  $T$ -depth of a circuit. In this work, we propose an automatic method that minimized the  $T$ -count, without a significant qubit overhead.

### C. Quantum oracle

A quantum oracle is defined as a “black box”  $2^{n+m+k} \times 2^{n+m+k}$  unitary operation  $U_f$  performing a multi-output Boolean function  $f: \{0, 1\}^n \rightarrow \{0, 1\}^m$ :

$$U_f : |x\rangle|y\rangle|0\rangle^k \mapsto |x\rangle|y \oplus f(x)\rangle|0\rangle^k \quad (2)$$

where  $|x\rangle$  represents the  $n$ -qubit input state,  $|y\rangle$  the  $m$  outputs, and  $|0\rangle^k$  are  $k$  qubits initialized to the state  $|0\rangle$ . A generic quantum circuit performing the unitary  $U_f$  is shown in Fig. 1. The extra  $k$  qubits are called ancillae and are used to store intermediate results for the computation of  $f$ . They must be restored to  $|0\rangle$  as only input and output states must be accessible at the end of the computation. Different automatic clean-up strategies are available in the literature [13], [18], exploring the trade-off between ancillae and operations.

#### D. Compute/uncompute property of Toffoli gates

We consider quantum circuits over the Clifford+ $T$  gate set. Our construction yields quantum circuits in an intermediate representation consisting of  $X = \text{NOT}$ ,  $\text{CNOT}$ , as well as Toffoli gates, which either consume or restore an ancilla and can therefore be implemented as follows [7]:

$$\begin{array}{c} |x_1\rangle \\ |x_2\rangle \\ |0\rangle \end{array} \begin{array}{c} \bullet \\ \bullet \\ \oplus \end{array} \begin{array}{c} |x_1\rangle \\ |x_2\rangle \\ |x_1x_2\rangle \end{array} = \begin{array}{c} |x_1\rangle \\ |x_2\rangle \\ |T\rangle \end{array} \begin{array}{c} \oplus \\ \oplus \\ \oplus \end{array} \begin{array}{c} \oplus \\ \oplus \\ \oplus \end{array} \begin{array}{c} T^\dagger \\ T^\dagger \\ T \end{array} \begin{array}{c} \oplus \\ \oplus \\ \oplus \end{array} \begin{array}{c} |x_1\rangle \\ |x_2\rangle \\ |x_1x_2\rangle \end{array} \begin{array}{c} \oplus \\ \oplus \\ \oplus \end{array} \begin{array}{c} H \\ H \\ S \end{array} \begin{array}{c} |x_1\rangle \\ |x_2\rangle \\ |x_1x_2\rangle \end{array} \quad (3)$$

$$\begin{array}{c} |x_1\rangle \\ |x_2\rangle \\ |x_1x_2\rangle \end{array} \begin{array}{c} \bullet \\ \bullet \\ \oplus \end{array} \begin{array}{c} |x_1\rangle \\ |x_2\rangle \\ |0\rangle \end{array} = \begin{array}{c} |x_1\rangle \\ |x_2\rangle \\ |x_1x_2\rangle \end{array} \begin{array}{c} \bullet \\ \bullet \\ \oplus \end{array} \begin{array}{c} |x_1\rangle \\ |x_2\rangle \\ |0\rangle \end{array} \begin{array}{c} \oplus \\ \oplus \\ \oplus \end{array} \begin{array}{c} Z \\ H \\ \uparrow \end{array} \begin{array}{c} |x_1\rangle \\ |x_2\rangle \\ |0\rangle \end{array} \quad (4)$$

In (3) the state  $|T\rangle = TH|0\rangle$  can be applied using magic-state distillation (see, e.g., [16]). The other three  $T$  gates in the circuit can be realized using magic-state distillation and gate teleportation (see, e.g., [19]).

In (4) the original state is recovered by measuring the third qubit and applying a controlled- $Z$  rotation (can be realized using 2  $H$  gates and a  $\text{CNOT}$  gate) to correct a  $-1$  phase due to the measurement back-action. In fact, we have

$$\begin{array}{c} |x_1\rangle \\ |x_2\rangle \\ |x_1x_2\rangle \end{array} \begin{array}{c} \bullet \\ \bullet \\ \oplus \end{array} \begin{array}{c} |x_1\rangle \\ |x_2\rangle \\ |0\rangle \end{array} = \begin{array}{c} |x_1\rangle \\ |x_2\rangle \\ |0\rangle \end{array} \begin{array}{c} \bullet \\ \bullet \\ \oplus \end{array} \begin{array}{c} |x_1\rangle \\ |x_2\rangle \\ |0\rangle \end{array} \begin{array}{c} H \\ Z \\ H \end{array} \begin{array}{c} |x_1\rangle \\ |x_2\rangle \\ |0\rangle \end{array} \quad (5)$$

and

$$\left. \begin{array}{c} |x_1\rangle \\ |x_2\rangle \\ |x_3\rangle \end{array} \right\} \begin{array}{c} \bullet \\ \bullet \\ \oplus \end{array} \begin{array}{c} |x_1x_2x_3\rangle \end{array} \cdot (-1)^{x_1x_2x_3} |x_1x_2x_3\rangle \quad (6)$$

If measuring the third qubit yields a 1 as a result, we must compensate the introduced  $-1$  phase. We can do so by applying a controlled- $Z$  gate, where  $Z = HXH$ .

Computing the Toffoli gate (logical-AND) requires 4  $T$  gates (see (3)), while uncomputing only requires Clifford gates (see (4)). This asymmetry is due to the fact that measurement is not reversible. It has been proven that a Toffoli gate cannot be computed with less than 4  $T$  gates [20]. Our proposed compilation approach is designed to maximally take advantage of this implementation, to reduce the number of  $T$  gates of the final circuit.

#### E. Logic networks

In this work, we are considering logic networks over the gate basis  $\{\wedge, \oplus, 1\}$ . In order to simplify our compiling algorithm, we allow our logic networks to have inverters. We can then propagate all uses of the constant 1 input to the outputs, since  $1 \oplus x = \bar{x}$ , and  $1 \wedge x = x$ , without increasing the number of AND gates. Consequently, the multiplicative complexity of a Boolean function over the gate set  $\{\wedge, \oplus, 1\}$  is the equivalent to the multiplicative complexity over the gate set  $\{\wedge, \oplus, \neg\}$  [5]. We use  $\bar{x}$  to denote the Boolean complement of  $x = 1 - x$ , and define  $x^0 = \bar{x}$  and  $x^1 = x$ .

We model a logic network for an  $n$ -variable Boolean function with inputs  $x_1, \dots, x_n$  as a Boolean chain with steps

$$x_i = x_{j(i)} \oplus x_{k(i)} \quad \text{or} \quad x_i = x_{j(i)}^{p(i)} \wedge x_{k(i)}^{q(i)}, \quad (7)$$

for  $n < i \leq n + r$ , depending on whether the step computes the XOR or the AND operation, where  $r$  is the number of steps. The constant values  $1 \leq j(i) < k(i) < i$  point to input or previous steps in the chain, and in the case of an AND gate Boolean constants  $p(i)$  and  $q(i)$  are used to possibly complement the gate's fan-in. The function value is computed by the last step  $f = x_{n+r}^p$ , which may be complemented. We write  $\circ_i = \wedge$ , if step  $i$  computes an AND gate, and  $\circ_i = \oplus$ , if step  $i$  computes an XOR gate. We define  $x_0 = 0$ , i.e., logic networks with no inputs and no steps represent the constant functions. The number of AND gates in the logic network is  $\tilde{c} = |\{i \mid \circ_i = \wedge\}|$ , which is an upper bound of the multiplicative complexity of the Boolean function it realizes.

**Example 1.** The majority-of-three function  $\langle x_1x_2x_3 \rangle = x_1x_2 \vee x_1x_3 \vee x_2x_3$  can be realized by the logic network

$$\begin{aligned} x_4 &= x_1 \oplus x_2, & x_5 &= x_2 \oplus x_3, \\ x_6 &= x_4 \wedge x_5, & x_7 &= x_2 \oplus x_6, \end{aligned}$$

with  $\tilde{c} = 1$ .

### III. COMPILATION ALGORITHM

In this section, we describe a synthesis algorithm that, given a logic network computing an  $n$ -variable Boolean function  $f(x)$ , finds a quantum circuit that implements the unitary operation

$$U_f : |x\rangle|y\rangle|0\rangle^{\tilde{c}} \mapsto |x\rangle|y \oplus f(x)\rangle|0\rangle^{\tilde{c}} \quad (8)$$

using  $4\tilde{c}$   $T$  gates. For the sake of clarity, we describe the single-output function case. Our actual implementation is a generalization of the described algorithm that also supports multi-output functions.

The key insight is that each AND gate in the logic network is driven by two multi-input parity functions of variables which are either inputs or AND steps in the logic network. Note that the arity of this multi-input parity functions might be 1. This is the case when the immediate input to an AND gate is a primary input or another AND gate itself. Formally, let the linear transitive fan-in of a node  $x_i$  in a logic network be defined using the recursive function

$$\text{ltfi}(x_i) = \begin{cases} \{x_i\} & \text{if } i \leq n \text{ or } \circ_i = \wedge, \\ \text{ltfi}(x_{j(i)}) \triangle \text{ltfi}(x_{k(i)}) & \text{otherwise,} \end{cases} \quad (9)$$

where ' $\triangle$ ' denotes the symmetric difference of two sets. It is easy to see that all elements in  $\text{ltfi}(x_i)$  are either inputs or steps that compute an AND gate.

**Example 2.** For the network in Example 1, we have

$$\begin{aligned} \text{ltfi}(x_4) &= \{x_1, x_2\} \\ \text{ltfi}(x_5) &= \{x_2, x_3\} \\ \text{ltfi}(x_6) &= \{x_6\} \\ \text{ltfi}(x_7) &= \{x_2, x_6\}. \end{aligned}$$

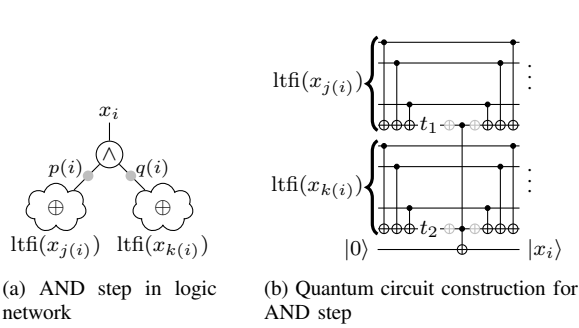


Fig. 2. Illustration of the general idea in which the fan-in nodes of an AND gate are considered as large XOR gates. These can be computed and uncomputed in-place in the quantum circuit using CNOT gates.

Algorithm 1 is based on this idea. Lines 21–24 show that the algorithm first computes all intermediate signals using the function ‘compute’ then copies the output to the qubit  $y$ , before restoring all ancilla qubits to  $|0\rangle$  by uncomputing ‘compute’. The function computes in lines 3–18 builds the circuit for each AND gate  $x_i$  as illustrated in Fig. 2.

**Input:** Logic network with gates  $x_{n+1}, \dots, x_{n+r}$

**Output:** Quantum circuit for  $U_f$

```

1 function compute is
2   for  $i = n + 1, \dots, n + r$  where  $\circ_i = \wedge$  do
3     set  $p \leftarrow p(i), q \leftarrow q(i), j \leftarrow j(i), k \leftarrow k(i)$ ;
4     set  $L_1 \leftarrow \text{ltfi}(x_j), L_2 \leftarrow \text{ltfi}(x_k)$ ;
5     if  $L_1 \subseteq L_2$  then
6       | swap  $L_1 \leftrightarrow L_2$  and  $p \leftrightarrow q$ ;
7     end
8     let  $t_1$  be some element in  $L_1 \setminus L_2$ ;
9     let  $t_2$  be some element in  $L_2$ ;
10    CNOT( $x, t_1$ ) for all  $x \in L_1 \setminus \{t_1\}$ ;
11    CNOT( $x, t_2$ ) for all  $x \in L_2 \setminus \{t_2\}$ ;
12    if  $p$  then NOT( $t_1$ );
13    if  $q$  then NOT( $t_2$ );
14    TOFFOLI( $t_1, t_2, x_i$ );
15    if  $p$  then NOT( $t_2$ );
16    if  $q$  then NOT( $t_1$ );
17    CNOT( $x, t_2$ ) for all  $x \in L_2 \setminus \{t_2\}$ ;
18    CNOT( $x, t_1$ ) for all  $x \in L_1 \setminus \{t_1\}$ ;
19  end
20 end
21 compute;
22 CNOT( $x_{n+r}, y$ );
23 if  $p = 0$  then NOT( $y$ );
24 compute†;

```

**Algorithm 1:** Heuristic compilation algorithm.

Note that we assume that  $L_1 \neq L_2$ . If this is not the case, it means that the functions computed by fan-in to the AND gate are equal, making the AND gate redundant. Also, note that the intersection of  $L_1$  and  $L_2$  may not be empty. Since we want to compute the value of  $L_1$  in-place on some signal  $t_1 \in L_1$ , we must ensure that  $L_1 \not\subseteq L_2$ . If the latter condition

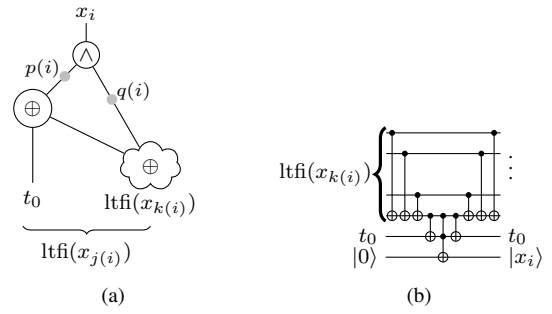


Fig. 3. Example in which one transitive fan-in is included in the other. The computed values can be reused.

applies, it is sufficient to swap  $L_1$  and  $L_2$ .

In addition, when  $L_2 \subseteq L_1$ , the value computed by  $L_2$  could be reused to compute  $L_1$ . This is achieved by modifying the elements in  $L_1$  such that  $L_1 = (L_1 \setminus L_2) \cup \{x_k\}$ . An example is shown in Fig. 3. In this case  $\text{ltfi}(x_j)$  includes  $\text{ltfi}(x_k)$  and  $\text{ltfi}(x_j) \setminus \text{ltfi}(x_k) = \{t_0\}$ . In general, when this optimization applies, it allows us to save  $2 \cdot |\text{ltfi}(x_k)|$  CNOT operations.

#### IV. PEBBLE STRATEGIES

In this section, we describe a dedicated SAT-based reversible pebbling strategy for logic networks over the basis  $\{\wedge, \oplus, \neg\}$ . A SAT-based reversible pebbling strategy allows us to reduce the number of qubits by trading off  $T$ -count. Compared to existing reversible pebbling strategies (see, e.g., [21], [18]), we enforce that all XOR operations are performed in-place.

The reversible pebble game is played on a logic network. Each node in a logic network can be assigned a pebble or not. We say that a node is pebbled, if it is assigned a pebble. At the beginning of the pebble game, at time step  $s = 0$ , all the primary inputs of the logic network are pebbled and all the gates are not. At each step a pebble can be put or removed from an AND gate, if both children are pebbled. For an XOR gate, the output can be pebbled, if both inputs are pebbled, but afterwards one of the input pebbles must be removed. This indicates that the result of the XOR computation (using a CNOT gate) has been computed into that input. All moves can be performed in a bidirectional way. Fig. 4 provides a summary. We allow multiple moves in a single step. The game is won when all output gates and all input nodes are pebbled, but all other nodes are not. Each pebble corresponds to a qubit that currently stores the computation result. Therefore, we are interested in the resource-constrained reversible pebble game in which at each step one can only use at most  $L$  pebbles.

We describe the SAT formula for the case in which the logic network drives a single output with gate  $x_{n+r}$ . The SAT formula has variables  $x_i^{(s)}$  for each node  $x_i$  and step  $0 \leq s \leq S$  in the network. The value of  $x_i^{(s)}$  encodes whether node  $x_i$  is pebbled at step  $s$ . Initially, all inputs are pebbled while all other nodes are not. At the last step  $S$ , the primary inputs and the output node must be the only nodes that are pebbled. These are enforced by the unit clauses

$$x_i^{(0)} \oplus [i > n] \quad (10)$$

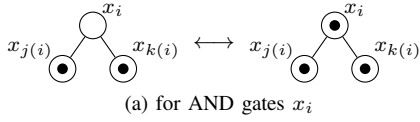
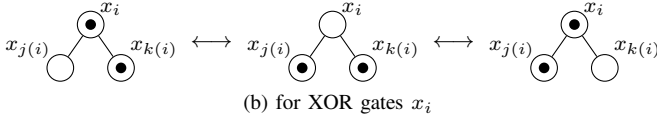
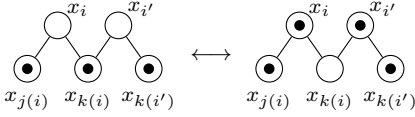
(a) for AND gates  $x_i$ (b) for XOR gates  $x_i$ 

Fig. 4. Pebble moves.

Fig. 5. Illegal XOR move for pair of XOR gates  $x_i$  and  $x_{i'}$ .

and

$$x_i^{(s)} \oplus [n < i < n + r] \quad (11)$$

for all  $1 \leq i \leq n+r$ , respectively, where  $[\cdot]$  denotes the Iverson bracket. For all gates  $x_i$  such that  $\circ_i = \wedge$ , the constraint

$$(x_i^{(s)} \oplus x_i^{(s+1)}) \rightarrow (x_{j(i)}^{(s)} \wedge x_{j(i)}^{(s+1)} \wedge x_{k(i)}^{(s)} \wedge x_{k(i)}^{(s+1)}) \quad (12)$$

ensures that the pebble of AND gate  $x_i$  can only change from time  $s$  to  $s+1$ , if all two children are pebbled in both time steps.

For all gates  $x_i$  such that  $\circ_i = \oplus$ , the constraints

$$(\bar{x}_i^{(s)} \wedge x_i^{(s+1)}) \rightarrow (x_{j(i)}^{(s)} \wedge x_{k(i)}^{(s)} \wedge (x_{j(i)}^{(s+1)} \oplus x_{k(i)}^{(s+1)})) \quad (13)$$

and

$$(x_i^{(s)} \wedge \bar{x}_i^{(s+1)}) \rightarrow ((x_{j(i)}^{(s)} \oplus x_{k(i)}^{(s)}) \wedge x_{j(i)}^{(s+1)} \wedge x_{k(i)}^{(s+1)}) \quad (14)$$

ensure the reversible pebble game semantics for XOR gates in Fig. 4(b).

Since we allow multiple moves at a single step, the current constraints so far allow illegal moves such as the one illustrated in Fig. 5. Here,  $x_i$  and  $x_{i'}$  are two XOR gates with a shared child  $x_{k(i)} = x_{j(i')}$ . We rule out such cases with explicit blocking constraints

$$\frac{(\bar{x}_i^{(s)} \wedge \bar{x}_{i'}^{(s)} \wedge x_c^{(s)} \wedge x_i^{(s+1)} \wedge x_{i'}^{(s+1)} \wedge \bar{x}_c^{(s+1)})}{(x_i^{(s)} \wedge x_{i'}^{(s)} \wedge \bar{x}_c^{(s)} \wedge \bar{x}_i^{(s+1)} \wedge \bar{x}_{i'}^{(s+1)} \wedge x_c^{(s+1)}), \quad (15)$$

where  $\circ_i = \circ_{i'} = \oplus$  and  $\{c\} = \{j(i), k(i)\} \cap \{j(i'), k(i')\}$  is the common child of gate  $x_i$  and  $x_{i'}$ .

All constraints described in (12)–(15) can easily be expressed as a CNF (conjunctive normal form). The final clause

$$\sum_{i=1}^{n+r} x_i^{(s)} \leq L \quad (16)$$

for each  $1 \leq s \leq S$  to restrict the number of used pebbles at each step  $s$  is translated into a CNF using cardinality

constraints (see, e.g., [22]). We employ a bounded-model checking style procedure using incremental SAT solving where we increase the maximum number of steps  $S$  until a solution is found, or terminate once a given resource limit is reached.

## V. EXPERIMENTAL RESULTS

In our experiments, we compile quantum oracles for functions represented by XAGs, targeting quantum circuits over the Clifford+ $T$  gate set. Our constructive algorithm and the SAT-based pebbling technique are implemented in the open-source C++ library for quantum compilation *caterpillar*<sup>1</sup>, that empowers *RevKit 3.1*<sup>2</sup>.

Our synthesis approach is capable of generating circuits with exactly  $4 \cdot \tilde{c}$   $T$  gates, where  $\tilde{c}$  is the number of AND nodes in the network. In cases in which the XAG implements the function with the minimum possible number of AND nodes ( $\tilde{c} = c_{\wedge}(f)$ ), our method returns a circuit with the minimum  $T$ -count. As indicated in Table I and II by ‘\*’, all the adders (whose XAGs are proven to have minimum multiplicative complexity [9]) are synthesized into circuits with the same  $T$ -count of the best-known manually designed circuits [7].

We compare against state-of-the-art methods that are also implemented in *RevKit 3.1*, synthesizing combinatorial circuits from the EPFL benchmarks,<sup>3</sup> both arithmetic and random control. In the results, we ignore Clifford gates as it is customary in fault-tolerant computing [4]. However, assuming that a  $T$  gate costs  $50\times$  as much as a Clifford gate, we would still have an overall gain compared to the state-of-the-art.

### A. Comparing to best-fit LUT-based synthesis

The first comparison is performed against the LUT-based hierarchical synthesis method *best-fit LHRS* [15].

Look-up table (LUT) mapping is a logic network decomposition technique widely used for logic circuit optimization [23]. A  $k$ -LUT mapping decomposes a logic network into  $k$ -feasible LUTs, i.e., single-output subnetworks with maximum  $k$  inputs. Hierarchical synthesis methods for quantum circuits use the LUT-mapping to decompose the design such that less scalable methods, e.g., ESOP-based synthesis [24], can be applied. This decomposition step defines the final number of qubits used by the circuit, that can be controlled by the parameter  $k$ . In fact, a large  $k$  will give fewer LUTs with more variables and, as a consequence, less qubits will be needed to store intermediate results. This procedure is typical of any LUT-based hierarchical method. In our experiment we set  $k$  to 16. The *best-fit* method uses an additional LUT mapping step for the synthesis of each sub-network. Thus allowing a reduced number of  $T$  gates with respect to similar techniques.

Our results show that the overhead in  $T$ -count that this method requires to reduce the number of qubits is too large, if compared with our technique, as shown in Table I. This is true,

<sup>1</sup><https://github.com/gmeuli/caterpillar>

<sup>2</sup><https://github.com/msoeken/revkit>

<sup>3</sup><https://lsi.epfl.ch/benchmarks>

especially considering that among the hierarchical methods, *best-fit* is the one returning the lowest number of  $T$  gates. Our results have in average about  $20.4\times$  smaller  $T$ -count, while the number of qubits is doubled. In the context of fault tolerant quantum computing, where the number of  $T$  gates is the predominant cost metric, our method outperforms the *best-fit* LUT-based method.

With our approach, the circuits count more Clifford gates. Nevertheless, if we consider the Clifford gates, together with the  $T$  gates, and accounting a 50:1 cost ratio, we still get that the LUT-based results are worst, in average, with respect to our approach. In addition, our current heuristic compilation technique is not exploiting shared logic among the CNOT gates, besides the extreme case discussed in Section III. A more careful analysis can lead to further CNOT gate count reduction.

### B. Comparing to hierarchical synthesis with Bennett clean-up

The second comparison we present is with respect to a state-of-the-art hierarchical method that uncomputes ancillae using the Bennett strategy [13]: nodes are synthesized in a bottom-up order, and uncomputation is performed in a top-down order. To make our comparison fair, we apply this method using XAG networks as inputs (a different network choice, e.g., and-inverter graphs, would lead to higher  $T$ -count). In addition, we modify this technique to also exploit the 4  $T$  gates quantum AND implementation (see Section II-D). This hierarchical method synthesizes a Toffoli gate for each AND node, two CNOT gates for each XOR node, and an  $X$  gate for each inversion, during computation and uncomputation. It results in circuits with the same minimum number of  $T$  gates achieved by our method. This minimum number is proportional to  $\tilde{c}$ —the number of AND nodes in the specification network. As shown in Table I, we achieve 70% fewer qubits on average. This is due to the strategy of computing XOR-blocks *in-place*, without using any ancilla as shown in Fig. 2.

### C. Minimized circuits with cryptography applications

With our compilation technique, we synthesize quantum oracles for Boolean functions used in a wide range of applications, from encryption to digital signatures, from hashing to error correction codes. The best-known version of these circuits, in terms of multiplicative complexity and depth, have been collected by the *Computer Security Resource Center* (CSRC) at the *National Institute of Standards and Technology* (NIST). Our results are shown in Table II. We synthesize: (i) finite field multiplication in  $GF(2^6)$  using irreducible polynomial  $x^6 + x^3 + 1$  (*mx6x31*), multiplication in  $GF(2^7)$  using irreducible polynomial  $x^7 + x^4 + 1$  (*mx7x41*) and using  $x^7 + x^3 + 1$  (*mx7x41*); (ii) binary multiplication with different input size  $n$  (*bm\_n*); (iii) a 16-bit and a 8-bit S-box (*s16*, *s8*); (iv) finite field multiplication in  $GF(2^8)$  using the

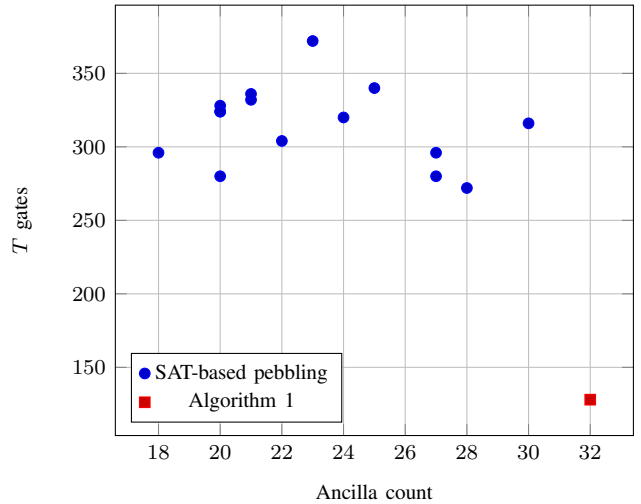


Fig. 6. Applying the SAT-based pebble strategy to the S-box benchmark.

AES polynomial  $x^8 + x^4 + x^3 + x + 1$  (*x8x4x31*). The benchmark circuits are available online.<sup>4</sup>

In addition, we evaluated our method on a set of circuits used in the context of *Multi-Party Computation* MPC and *Fully Homomorphic Encryption* FHE, optimized for the number of AND gates using the technique proposed in [10]. Oracles for these functions can be used to evaluate the cost of a Grover’s attack over the relative encryption scheme. In fact, it has been shown how Grover’s algorithm can be used as the quantum version of a key attack, if the quantum circuit for the encryption function is known [25]. From the benchmarks available online<sup>5</sup> we synthesize: (i) block ciphers AES and DES in their expanded and non expanded variant, the latter meaning that the input key is assumed non-expanded; (ii) arithmetic functions such as adders, multipliers, and comparators.

### D. Evaluating the pebble strategies for the S-box

In this section, we evaluate the effect of the proposed SAT-based pebbling strategy discussed in Section IV. We implemented the SAT-based pebbling algorithm in Q# [26] with Z3 [27] as SAT solving backend. As benchmark, we use the 8-bit S-box described in the previous section (*s8*). We apply our compilation algorithm (Alg. 1) to obtain a reference quantum circuit. Since its XAG representation requires 32 AND gates, using the proposed heuristic compilation algorithm we can achieve a quantum circuit with 32 ancilla lines and 128  $T$  gates (note that 16 more qubits are required for storing inputs and outputs). We use the SAT-based pebbling strategy with different values for  $L$  (number of maximum ancillae) and different random seeds to obtain various other quantum circuits with fewer number of ancilla lines.

The results are plotted in Fig. 6. As can be seen, the SAT-based pebbling approach can find various different

<sup>4</sup><http://cs-www.cs.yale.edu/homes/peralta/CircuitStuff/CMT.html>

<sup>5</sup><https://homes.esat.kuleuven.be/~nsmart/MPC/>

TABLE I  
COMPARISONS

					Best-fit lhrs [15]				Bennett				Proposed			
	I	O	XOR	AND	qubits	T	Clifford	t[s]	qubits	T	Clifford	t[s]	qubits	T	Clifford	t[s]
adder	256	129	549	128	448	14411	319	0.0	933	512	1938	0.0	385	512*	1778	0.0
arbiter	256	129	0	1181	694	134492	1297	0.1	1437	4724	1	0.1	1437	4724	1	0.1
bar	135	128	1728	832	863	44800	1328	0.1	2695	3328	6656	0.4	1032	3328	23552	0.3
cavlc	10	11	197	494	123	59650	430	0.0	701	1976	788	0.0	504	1976	600	0.1
ctrl	7	26	8	85	36	4102	21	0.0	101	340	41	0.0	93	340	21	0.0
dec	8	256	0	341	293	30061	58	0.0	349	1364	0	0.0	349	1364	0	0.0
div	128	128	8994	6060	4188	248739	10044	1.1	15182	24240	35891	13.7	6188	24240	260301	14.2
i2c	147	142	502	623	377	65674	604	0.0	1273	2492	2041	0.1	771	2492	1247	0.1
int2float	11	7	101	100	44	8645	104	0.0	212	400	405	0.0	111	400	345	0.0
log2	32	32	9371	19436	8192	2177089	28176	4.4	28839	77744	37437	46.5	19469	77744	965225	65.3
max	512	130	1479	931	1076	82287	2265	0.1	2922	3724	5658	0.4	1444	3724	9060	0.4
mem_ctrl	1204	1231	4168	5113	3397	498240	5206	0.3	10486	20452	15899	4.1	6319	20452	12077	5.6
multiplier	128	128	8614	11940	5294	839571	21330	1.8	20682	47760	34269	24.4	12069	47760	869535	39.5
priority	128	8	158	327	256	65563	571	0.0	613	1308	633	0.0	455	1308	467	0.0
router	60	30	0	96	90	7930	93	0.0	157	384	27	0.0	157	384	27	0.0
sin	24	25	1770	4075	1531	392926	5881	0.3	5869	16300	7046	2.0	4099	16300	62330	3.5
sqrt	128	64	9640	6244	4297	375639	19207	1.2	16012	24976	38609	14.5	6372	24976	207921	15.1
square	64	128	8084	5181	3967	262544	8905	1.0	13330	20724	32154	10.0	5246	20724	247002	8.6
voter	1001	1	6066	5651	2640	274431	7084	0.3	12718	22604	24265	7.9	6652	22604	168081	9.5
<b>Normalized geometric mean</b>					<b>0.5</b>	<b>20.4</b>			<b>1.7</b>	<b>1</b>			<b>1</b>	<b>1</b>		

\* matches best-known  $T$ -count [7].

TABLE II  
BENCHMARKS FROM CRYPTOGRAPHY

	I	O	XOR	AND	qubits	Clifford	T	t[s]
bm_10	20	19	102	52	89	770	208	0.0
bm_11	22	21	108	78	119	716	312	0.0
bm_12	24	23	126	81	120	908	324	0.0
bm_15	30	29	195	117	174	1776	468	0.0
bm_20	40	39	314	208	279	3154	832	0.0
bm_30	60	59	687	351	452	8756	1404	0.1
bm_40	80	79	1079	624	759	15618	2496	0.2
bm_50	100	99	1847	676	855	32354	2704	0.3
bm_60	120	119	2253	1053	1262	41324	4212	0.5
bm_70	140	139	2985	1432	1643	54036	5728	0.8
bm_80	160	159	3494	1872	2151	73570	7488	1.4
bm_90	180	179	4561	1989	2318	105578	7956	1.6
bm_100	200	199	5143	2704	3063	129810	10816	2.7
mcustom	16	8	79	27	51	424	108	0.0
mx6x31	12	6	30	27	45	132	108	0.0
mx7x41	14	7	44	40	61	156	160	0.0
mx7x41	14	7	45	40	61	168	160	0.0
s16	17	16	333	113	146	7049	452	0.0
s8	8	8	83	32	48	1408	128	0.0
x8x4x31	16	8	69	48	72	370	192	0.0
adder_32bit	64	33	150	32	97	556	128*	0.0
adder_64bit	128	65	284	64	193	1132	256*	0.0
AES-expanded	1536	128	20325	5440	6979	1583232	21760	14.2
AES-non-expanded	256	128	25124	6800	7059	3009160	27200	22.2
comp_32bit_sign_LT	64	1	116	108	172	312	432	0.0
comp_32bit_sign_LTEQ	64	1	89	114	178	265	456	0.0
DES-expanded	832	64	11263	15126	15959	256441	60504	69.4
DES-non-expanded	128	64	11105	15093	15222	246564	60372	68.7
mult-32x32	64	64	2473	4107	4172	54498	16428	3.0

\* matches best-known  $T$ -count [7].

quantum circuits with 18–30 required ancillae. However, the  $T$ -count increases, as AND gates are computed and uncomputed more than once. Note that in the described SAT-based pebbling strategy we do not constrain the number of AND operations. A weighted pebble game in which computations of AND gates are more expensive than computations of XOR gates can help to find solutions with

fewer  $T$  gates, however, it comes with an overhead in solving time. Besides the (red) data point obtained by the heuristic compilation algorithm, there are 3 more Pareto optimal solutions, namely (18, 296), (20, 280), and (28, 272). While all solutions were found within a few seconds, we noticed that the SAT-based pebbling strategy does not yet scale well to larger benchmarks such as the EPFL benchmarks. We plan to investigate ways to make SAT-based pebbling more scalable in future works.

## VI. FUTURE WORK

In this work we propose XAGs as advantageous multi-level logic representations that allow automatic compilation to reach performances similar to manual methods. We have mostly focused on XAGs with minimal number of AND nodes, proportional to our proposed upper bound for the number of qubits and  $T$ -count of the final circuit. In future works, we aim at focusing on the impact of the number of XOR nodes in the graph. In fact, an XOR block of  $x$  variables, requires  $2 \times (x - 1)$  CNOT gates to be computed and uncomputed once (see Fig. 2). Techniques can be borrowed from multi-level logic optimization to minimize the number of XOR nodes [28], [11] without increasing the number of ANDs and consequently minimize the number of CNOTs in the final circuit.

In addition, it is possible to combine our method with post-synthesis CNOT optimization techniques, either heuristic [29], [30] or exact [31], to reduce the CNOT overhead.

We present a pebbling strategy technique specifically designed to work on XAGs, where each XOR can be computed in-place, while AND nodes must be computed out-of-place. The technique can be improved by implementing a weighted pebbling game, where pebbling/unpebbling AND nodes is penalized with respect to XOR nodes.



## VII. CONCLUSION

We presented a new heuristic compilation algorithm for quantum oracles which addresses fault-tolerant quantum computing, minimizing the  $T$ -count. In our method, the number of  $T$  gates depends on the number of AND gates used to represent the Boolean function  $f$  as an XAG. The algorithm suggests a new upper bound on the  $T$ -count that is proportional to the multiplicative complexity of the function  $f$ , namely  $4c_{\wedge}(f)$ . Future research on multiplicative complexity will not only influence results in cryptography, but also in quantum computing, thanks to the direct correlation between of the multiplicative complexity of Boolean functions and the number of  $T$  gates and ancillae in the corresponding quantum circuit.

Our technique achieves better results compared to other state-of-the-art automatic compilers. In fact, these either produce too many  $T$  gates, or they rely on a larger number of qubits. Nowadays, the research community is making many efforts to develop a scalable quantum technology, capable of producing quantum systems characterized by a large number of qubits. Fault tolerant quantum computing will only be possible when this technology progress is achieved. For this reason, it will be paramount to control the number of  $T$  gates, rather than the number of qubits. As a consequence, compilation methods that result in large  $T$ -counts should be discarded in favor of low  $T$ -count methods.

Finally, we provide synthesis statistics for two benchmarks containing useful designs in the context of cryptography which can be useful for deriving resource cost estimates for quantum-based cryptanalysis.

*Acknowledgments:* This research was supported by the Swiss National Science Foundation (200021-169084 MAJesty).

## REFERENCES

- [1] L. K. Grover, "A fast quantum mechanical algorithm for database search," in *Symposium on Theory and Computing*, 1996, pp. 212–219.
- [2] P. W. Shor, "Polynomial-time algorithms for prime factorization and discrete logarithms on a quantum computer," *SIAM Journal on Computing*, vol. 26, no. 5, pp. 1484–1509, 1997.
- [3] A. W. Harrow, A. Hassidim, and S. Lloyd, "Quantum algorithm for linear systems of equations," *Phys. Rev. Lett.*, vol. 103, 2009.
- [4] M. Amy, D. Maslov, M. Mosca, and M. Roetteler, "A meet-in-the-middle algorithm for fast synthesis of depth-optimal quantum circuits," *IEEE Trans. on CAD of Integrated Circuits and Systems*, vol. 32, no. 6, pp. 818–830, 2013.
- [5] J. Boyar, R. Peralta, and D. Pochuev, "On the multiplicative complexity of boolean functions over the basis  $(\wedge, \oplus, 1)$ ," *Theoretical Computer Science*, vol. 235, no. 1, pp. 43–57, 2000.
- [6] C. Jones, "Low-overhead constructions for the fault-tolerant Toffoli gate," *Physical Review A*, vol. 87, no. 2, p. 022328, 2013.
- [7] C. Gidney, "Halving the cost of quantum addition," *Quantum*, vol. 2, p. 74, 2018.
- [8] M. G. Find, "On the complexity of computing two nonlinearity measures," in *Int'l Computer Science Symposium in Russia*, 2014, pp. 167–175.
- [9] J. Boyar and R. Peralta, "Tight bounds for the multiplicative complexity of symmetric functions," *Theoretical Computer Science*, vol. 396, no. 1–3, pp. 223–246, 2008.
- [10] E. Testa, M. Soeken, L. Amarú, and G. De Micheli, "Reducing the multiplicative complexity in logic networks for cryptography and security applications," in *DAC*, 2019.
- [11] J. Boyar, P. Matthews, and R. Peralta, "Logic minimization techniques with applications to cryptology," *Journal of Cryptology*, vol. 26, no. 2, pp. 280–312, 2013.
- [12] Ç. Çalik, M. S. Turan, and R. Peralta, "The multiplicative complexity of 6-variable Boolean functions," *Cryptography and Communications*, vol. 11, no. 1, pp. 93–107, 2019.
- [13] C. H. Bennett, "Time/space trade-offs for reversible computation," *SIAM Journal on Computing*, vol. 18, no. 4, pp. 766–776, 1989.
- [14] M. Soeken, M. Roetteler, N. Wiebe, and G. De Micheli, "Hierarchical reversible logic synthesis using LUTs," in *Design Automation Conference*, 2017, pp. 78:1–78:6.
- [15] G. Meuli, M. Soeken, M. Roetteler, N. Wiebe, and G. De Micheli, "A best-fit mapping algorithm to facilitate ESOP-decomposition in Clifford+ T quantum network synthesis," in *Asia and South Pacific Design Automation Conference*. IEEE Press, 2018, pp. 664–669.
- [16] S. Bravyi and A. Kitaev, "Universal quantum computation with ideal Clifford gates and noisy ancillas," *Physical Review A*, vol. 71, p. 022316, 2005.
- [17] J. O’Gorman and E. T. Campbell, "Quantum computation with realistic magic-state factories," *Physical Review A*, vol. 95, no. 3, p. 032338, 2017.
- [18] G. Meuli, M. Soeken, M. Roetteler, N. Bjorner, and G. De Micheli, "Reversible pebbling game for quantum memory management," in *Design, Automation and Test in Europe*, 2019.
- [19] D. Gottesman and I. L. Chuang, "Quantum teleportation is a universal computational primitive," *Nature*, vol. 402, pp. 390–393, 1999.
- [20] M. Howard and E. Campbell, "Application of a resource theory for magic states to fault-tolerant quantum computing," *Phys. Rev. Lett.*, vol. 118, 2017.
- [21] A. Parent, M. Roetteler, and K. M. Svore, "REVS: A tool for space-optimized reversible circuit synthesis," in *Int'l Conf. on Reversible Computation*, 2017, pp. 90–101.
- [22] D. E. Knuth, *The Art of Computer Programming, Volume 4, Fascicle 6: Satisfiability*. Addison-Wesley, 2015.
- [23] A. Mishchenko, S. Chatterjee, and R. Brayton, "DAG-aware AIG rewriting: a fresh look at combinational logic synthesis," in *Design Automation Conference*, 2006.
- [24] K. Fazel, M. A. Thornton, and J. Rice, "ESOP-based toffoli gate cascade generation," in *Pacific Rim Conference on Communications, Computers and Signal Processing*, 2007.
- [25] M. Grassl, B. Langenberg, M. Roetteler, and R. Steinwandt, "Applying grover’s algorithm to AES: quantum resource estimates," in *Post-Quantum Cryptography*, 2016.
- [26] K. Svore, A. Geller, M. Troyer, J. Azariah, C. Granade, B. Heim, V. Kliuchnikov, M. Mykhailova, A. Paz, and M. Roetteler, "Q#: Enabling scalable quantum computing and development with a high-level DSL," in *Real World Domain Specific Languages Workshop*, 2018, pp. 7:1–7:10.
- [27] L. M. de Moura and N. Bjorner, "Z3: an efficient SMT solver," in *Int'l Conf. on Tools and Algorithms for the Construction and Analysis of Systems*, 2008, pp. 337–340.
- [28] C. Fuhs and P. Schneider-Kamp, "Synthesizing shortest linear straight-line programs over GF(2) using SAT," in *Int'l Conf. on Theory and Applications of Satisfiability Testing*, 2010, pp. 71–84.
- [29] Y. Nam, N. J. Ross, Y. Su, A. M. Childs, and D. Maslov, "Automated optimization of large quantum circuits with continuous parameters," *npj Quantum Information*, vol. 4, no. 23, pp. 1–12, 2018.
- [30] M. Amy, P. Azimzadeh, and M. Mosca, "On the CNOT-complexity of CNOT-phase circuits," *arXiv preprint arXiv:1712.01859*, 2017.
- [31] G. Meuli, M. Soeken, and G. De Micheli, "SAT-based {CNOT, T} quantum circuit synthesis," in *Int'l Conf. on Reversible Computation*. Springer, 2018, pp. 175–188.